Flame stabilization using a plasma discharge in a lifted jet flame

3 authors:

Wookyung Kim
United Technologies Research Center
28 PUBLICATIONS   710 CITATIONS

SEE PROFILE

Godfrey Mungal
Stanford University
223 PUBLICATIONS   6,870 CITATIONS

SEE PROFILE

Mark A. Cappelli
Stanford University
432 PUBLICATIONS   4,852 CITATIONS

SEE PROFILE

Some of the authors of this publication are also working on these related projects:

Propulsion Plasma Diagnostics View project

Glew Doctoral Research at Stanford University View project

Flame stabilization using a plasma discharge in a lifted jet flame

W. Kim[*], M.G. Mungal[†] and M.A. Cappelli[‡]
Stanford University, Stanford, CA, 94305-3032

Stable combustion in a harsh environment, such as lean fuel concentration and/or low temperature conditions, is attractive because of its low emissions. However, such flames suffer from lack of stability. In our research, an AC plasma discharge is applied to a lifted jet flame to increase the stability of the flame. Two types of discharges are utilized for this experiment. First, a single electrode diffuse discharge (SEDD) directly to the liftoff flame base is investigated. Second, a dielectric barrier discharge (DBD) is achieved by adding a quartz coated secondary electrode. To quantify the stability, we measure the jet velocity and coflow velocity corresponding to liftoff and/or blowout points for both cases. We find that addition of a very small amount of energy (less than 0.01% of the energy of main system) to the flow in the form of these types of discharges significantly improves the flame stability. For example, we observe that the SEDD increases the liftoff stability limit by 30% in terms of coflow speed. In addition, it shows a self-adjusting feature of the discharge angle such that the stabilization can be achieved regardless of orientation and location of the electrode over a relatively broad range of conditions. In case of DBD, we find a more intense stabilization effect, 50% of the improvement in terms of coflow speed, than the single electrode discharge as well as a self-ignition ability, which is not found in the first type of discharge. In addition, we believe that the essential characteristic of the non-equilibrium state of the DBD due to its short pulse duration enables the targeting of energy deposition in an efficient way.

I.   Introduction

Flame stabilization has been, and continues to be, one of the critical issues in stationary/aero gas turbines, industrial burners, engines and other practical combustion related devices. Moreover, the increasing demand for lean combustion in efforts to decrease NO_x formation further complicates the issue and provides a harsher challenge in achieving a stabilized flame.

Several major methods have been proposed to achieve stabilization in combustion flames: use of pilot flames, bluff bodies and swirl. Pilot flames often utilize hydrogen and have been implemented to stabilize laboratory scale, non-premixed flames[1,2]; an equivalent concept may also be applied using an oxygen pilot flame. Another method of stabilization uses pure oxygen coflow surrounding a jet flame, and has been used in laboratory–scale diffusion flames[3]. However, these methods have shortcomings in their practical applicability to industry due to the added complexity of the overall system. Bluff bodies or swirl stabilization mechanisms have been exploited both in premixed and partially premixed flames to generate a recirculation zone which preheats the reactants, resulting in flame stability[4]. However, increasing entrainment of high temperature burned gas into the fresh reacting jet by recirculation along with longer residence time of flow in the reaction region by a swirling motion can also lead to significant increase in the formation of NO_x. Also, as in the case of a pilot flame, these two methods have an intrinsic limit in that main energy transfer occurs predominantly in the form of thermal energy, which implies that a portion of it is lost while local thermal equilibrium is established[5].

Flame stabilization through the use of a plasma generated by an electrical discharge might allow a more practical and efficient means in comparison to the previously mentioned methods, while promoting the advantages of on-

---

[*] Graduate Research Assistant, Mechanical Engineering, AIAA Student Member.
[†] Professor, Mechanical Engineering, AIAA Associate Fellow.
[‡] Associate Professor, Mechanical Engineering, AIAA Member.

1
American Institute of Aeronautics and Astronautics

demand capability, portability and avoidance of pilot gases. It is, however, important that the discharge device and equipment used for plasma generation be relatively simple[6, 7]and easy to integrate into the combustor design. Also, if the discharge time scale is small in comparison to the characteristic time scales of a particular combustion system, such as the flow and/or chemical time scales, then active feedback control is possible. Also, controllable parameters such as voltage, frequency and duration for non-DC discharges can be more precisely adjusted in comparison to that of a conventional flow control mechanism.

The main benefit of a plasma discharge compared to other more widely used methods is that it can be designed to target a specific energy mode corresponding to the major energy transfer path in a non-equilibrium condition. To achieve a non-equilibrium state, one needs to restrict energy transfer from internal (electronic, rotational or vibrational) energy modes to translational energy modes. The simplest way to achieve this is to limit the time scale of the discharge, so that discharge duration becomes much shorter than the time scale of energy transfer to (and amongst) the other modes. A short duration can be achieved in a number of different ways. Some methods discussed in the literature include the use of so-called AC Dielectric Barrier Discharges, or DBDs, which are self-extinguishing discharges resulting from the counter electric field generated by charge accumulation on a high capacitance material between conductive electrodes[8]. Others include the use of physically restricted discharges, such as micro-scale discharge arrays[9, 10] (e.g., Micro-Hollow Cathode Discharges, or MHCD), or ultra short pulse discharges, which utilize a special, high voltage, nanosecond pulse generator circuit that can forcefully interrupt a high input voltage[11]. An advantage of a DBD is that it requires minimal experimental effort to implement and integrate into a combustion facility, and provides relatively short discharge durations with an off-the-shelf, affordable AC power supply. A MHCD, while it is considered an effective discharge source of electrons, has the drawback that the manufacturing of the electrodes is complicated by scaling issues. While a nanosecond pulse generator circuit provides controllable and repeatable pulsed discharges, these discharge power supplies are quite complicated and expensive, and are very sensitive to proper impendence matching of the supply to the discharge load..

The advantages and practicability offered by the DBDs warrant their investigation as possible methods as flame stabilization enhancers. In this study, we shall report on preliminary results obtained in the stabilization of flames with a dielectric barrier discharge. In addition, however, we discovered that with a DBD, we see the presence of a secondary diffuse (non-filamentary) discharge from the AC driven bare electrode directly to the flame. This alternative discharge is also examined as a potential stabilization enhancer. We will refer to this alternative discharge configuration as a 'Single Electrode Diffuse Discharge', or SEDD, in this paper. The advantages and stabilization performance of a SEDD are addressed in later sections of this paper.

The scope of this work is focused on the stabilization of lifted jet methane flames. Currently, it is believed that the natural stabilization mechanism of a lifted jet flame is a leading edge flame of triplet character for both laminar and turbulent jets, which implies that the flame base is anchored on a triple point of three branches where competition occurs between flame propagation speed and local flow velocity[12, 13]. This perspective matches well to our previous observations in which the lifted flame base is located in a flow field whose local flow velocity is two to three times that of the laminar flame speed[14] (S_L). Therefore, the lifted jet flame is considerably more difficult to stabilize over 2~3 S_L of <u>coflow</u> speed regardless of velocity of the jet[15]. Thus, in the current work, we use coflow speed as one of the main criteria to evaluate the degree of improvement of discharge-aided flame stabilization as well as another generally accepted stabilization criteria, namely the jet velocity.

II.   Experimental Setup

A schematic diagram of the experimental setup is provided in Fig. 1. A lifted methane jet flame is formed in a vertical wind tunnel whose cross section dimensions are 30x30cm. A nozzle with inner diameter of 4.6mm is oriented parallel to the flow direction (jet in coflow). Coflow speed is measured by a PIV system while jet velocity is determined by measuring pressure and volume flow rate at the upstream using flowmeters. The PIV system consists of a 15 Hz, double exposure interlaced CCD camera (Kodak ES 1.0), 15 Hz double pulse 2nd harmonic Nd:YAG laser (Spectraphysics PIV-400) and an alumina particle seeding system. Also, an ICCD camera (Princeton instrument PI-MAX) which has 50 kHz maximum gating frequency and 1.5nm minimum gating width is used to visualize the discharge in a time resolved manner. Information on voltage and current at the electrode is collected by a high voltage probe (Tektronics P6015A) with a voltage reduction ratio of 1/1000, and Rogowski coil (Pearson Electronics, model 2877) respectively, and recorded onto a high-speed digital oscilloscope (Tektronics TDS 7104). In addition, we record intrinsic plasma emission with a spectrometer that has a spectral resolution of 0.17 nm (Ocean optics S2000). As a discharge power source, we use an affordable and easy-to-implement AC power supply (Information Unlimited PVM300) with open circuit peak voltage of 20 kV and typical frequency range of 25~35
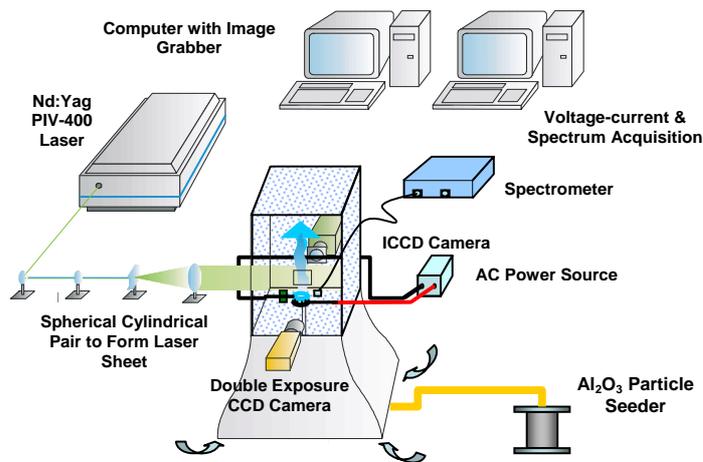
Figure 1 Schematic of the experimental setup.

kHz. Finally, a platinum electrode (driven electrode) and a pair of platinum/quartz coated platinum electrodes are used for SEDD and DBD respectively. For the SEDD, the powered line of an AC power source is connected to the bare platinum electrode (driven electrode) while the other reference line from the power supply is grounded to a common ground with the wind tunnel. For the DBD, the platinum electrode is powered while the quartz-coated electrode is permanently grounded. A detailed description of the electrode shape and configuration is described in the following section.

III. Results and Discussion

A. Electrode Design

Figure 2 shows the evolution of our electrode design as studied chronologically. Our initial design was a simple point-to-point discharge between metal electrodes (Fig. 2a). In tests however, we observed very intense glow-to-arc transitions, even at modest voltages. This phenomenon is expected in high pressure and low temperature gases, even with pulse widths down to a few tens of nanoseconds- much shorter than the relevant timescales of our experimental conditions. This transition is problematic in that it may create a "thermal" plasma with a high local gas temperature not unlike that created by a conventional ignition spark plug. Operation in this mode also requires the aggressive cooling of the electrodes to prevent melting. As a next configuration, we coated one of the single point electrodes with a dielectric material such as thermocouple insulation (99.8% of alumina, Fig. 2b) or a thin sapphire slide. These two materials have a relatively high melting point (> 2200K) and a relatively high dielectric constant (~ 10), allowing them to endure the high temperature flame environment and provide a strong counter electric field due to charge accumulation within the AC cycle. However, this configuration was difficult to conform to the axisymmetric geometry of the flame. Furthermore, this geometry/configuration tended to disturb the jet flow since

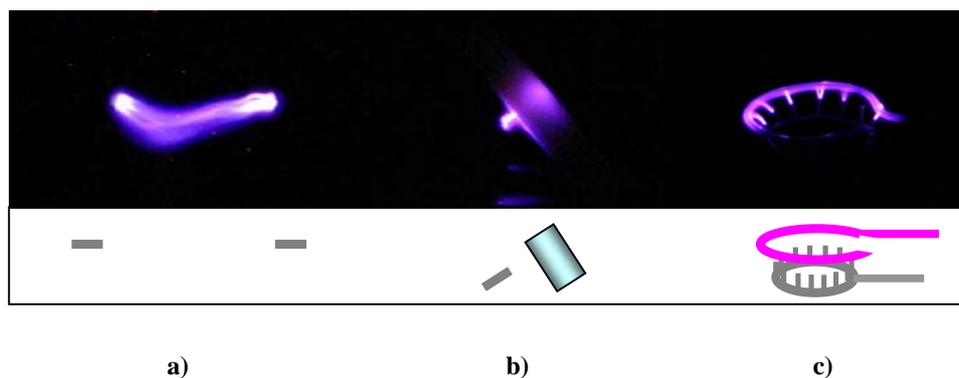

a)   b)   c)

Figure 2 Evolution of the discharges and electrode design. a) shows point-to-point discharge between metal electrodes, b) represents Dielectric Barrier Discharge (DBD) from a platinum electrode to an alumina cylinder which surrounds the second platinum electrode, c) illustrates DBD in round geometry electrodes; a lower electrode and its tips are made of platinum and an upper electrode is quartz covered. Schematics of the physical shapes are provided underneath each discharge picture.
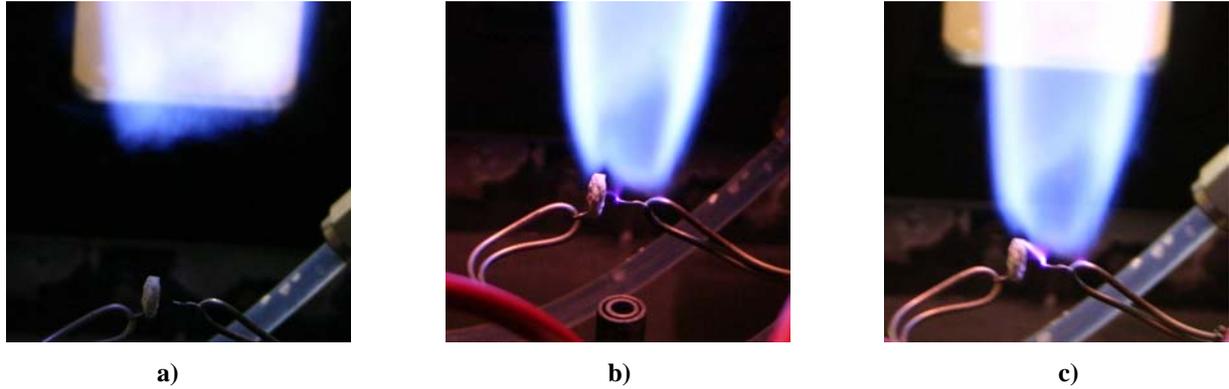
| a) | b) | c) |

Figure 3 Preliminary observations of discharge-aided flame stabilization. a) No voltage, b) Moderate voltage and c) High voltage. It is shown that a flame is lifted off in a) and reattached by discharges in b). SEDD as well as DBD are observed in b) and unintentional arc transitions are observed in c) due to high input voltage. The electrode position is 10 diameters (46mm) above the nozzle.

the discharge length scale (separation between the electrodes), typically 2 mm, was smaller than the diameter of the jet (> 4.6mm).

To mitigate these problems, we designed a circumferential powered (bare) electrode the diameter of which is approximately 25 mm and on which we welded several platinum tips which serve to increase the electric field (Fig. 2c). For DBD experiments, we also fabricated a circumferential grounded-electrode of diameter slightly larger than the powered (bare) electrode. This grounded electrode was threaded within a quartz tube to provide the dielectric barrier. In this electrode pair configuration we can sustain a plasma that has a discharge direction almost parallel with the flow, conforming with the jet symmetry and also minimizing disturbances to the jet flow. Figure 2c shows the final electrode design. For the SEDD studies, the grounded quartz-covered electrode was removed from the flow, and the flame itself serves as a virtual ground for the discharge.

B. Preliminary Experiments for Parameter Evaluation

Figure 3 illustrates an example of an AC discharge between a bare platinum electrode and sapphire covered platinum electrode. In Fig. 3a, a lifted flame (in the absence of a discharge) is located approximately 50mm above the electrode pair, which itself is located 46mm downstream of the jet nozzle. Once the discharge is initiated, the flame is pulled down and held close next to the electrode (Fig. 3b). It is apparent in this figure, that there are two distinct discharge kernels: a relatively intense discharge between the electrodes (DBD), and a diffuse discharge from
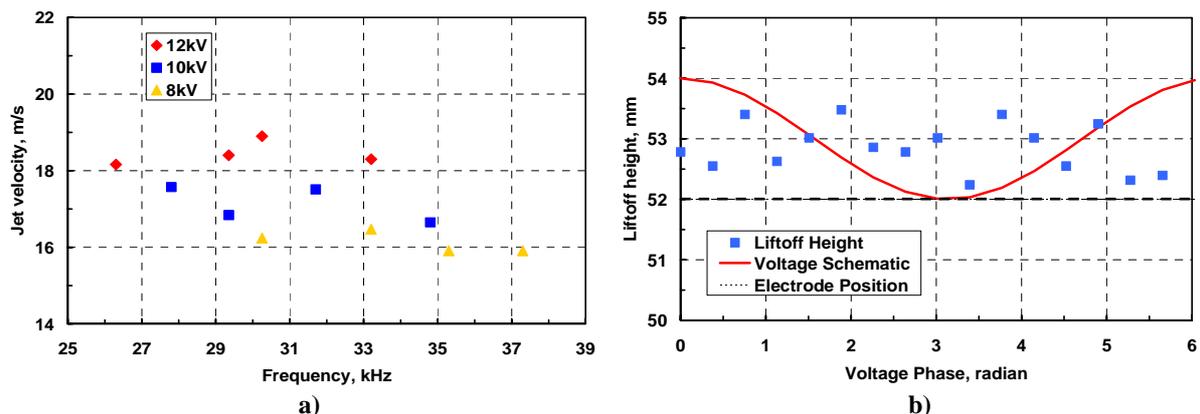

| a) | b) |

Figure 4. Parameter evaluations. a) Liftoff jet velocity vs. input frequency in DBD mode with 46mm electrode height. b) Liftoff height vs. input phase in SEDD. As shown, the frequency and phase of the input voltage are not critical factors to determine the liftoff condition. The black dotted line in b) represents electrode position and red curve shows voltage schematic. Coflow speed is 0.42m/s (1.1S_L) in a) and b) while jet velocity and peak-to-peak input voltage in b) are 10.5m/s and 10kV, respectively.
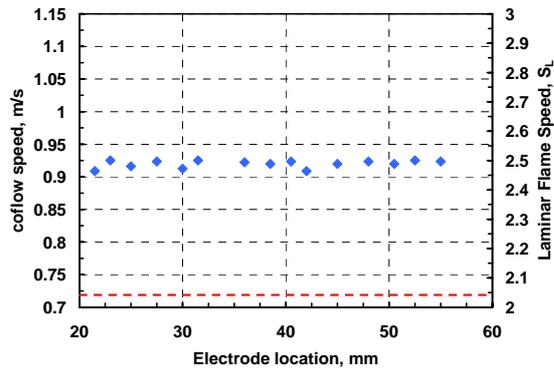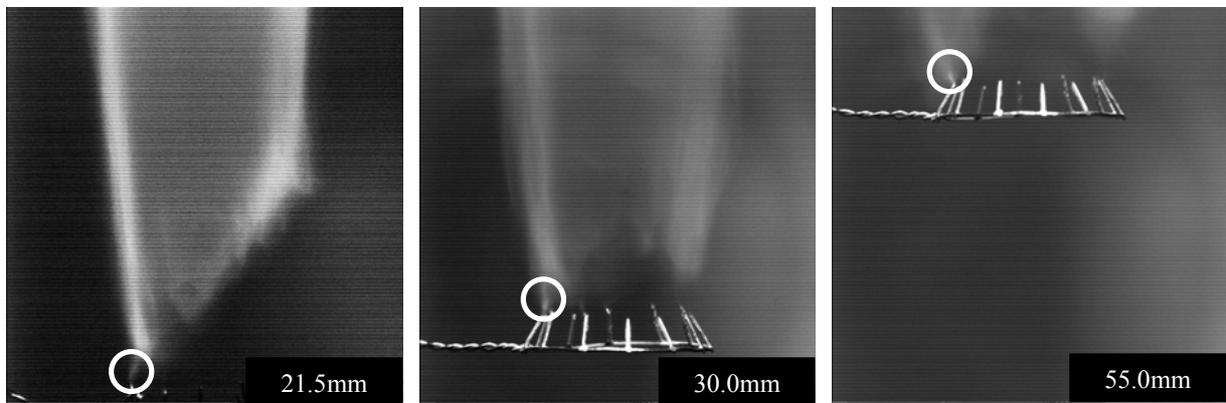
Figure 5. Liftoff coflow speed as a function of electrode position. In a), the coflow speed is insensitive to electrode position in the SEDD mode. For comparison, the coflow speed in no discharge condition is shown as a dotted line. Coflow speed is expressed in terms of laminar flame speed as well as physical value. In b), the change of discharge angles (inside of white circles) is illustrated for different electrode positions. Electrode positions are noted in each picture. For all cases, the jet velocity is 10.5m/s, and Re_d is 2955.

the bare platinum electrode tip to the flame base (SEDD). We believe that the high temperature flame environment serves as a virtual electrode as it acts as a large reservoir of charged particles and has a finite bulk capacitance.

Figure 3c is an example of an unintentional glow-to-arc transition when an excessive voltage (9 kV peak-to-peak) is applied. In this photograph, an intense arc kernel is seen between the electrodes, while a brighter and wider emission is observed between the arc kernel near the platinum tip and the flame base. This glow-to-arc transition is easily detected by the acoustic emission generated at the frequencies of the power supply. The transition is also characterized by an increased discharge current. The transition can be suppressed by utilizing an improved dielectric barrier, as is the case with our final circumferential electrode design described in the previous section.

In these preliminary experiments, we also examined the dependence of parameters such as the AC supply frequency and the positioning of the electrodes on variables such as the coflow speed and jet velocity. In Fig. 4a, the dependence of the liftoff jet velocity on the input frequency with a fixed coflow speed and electrode positioning in the DBD mode is illustrated. It can be seen that increasing the supply frequency has a negligible influence on the liftoff jet velocity over the range of conditions studied. However, increasing the voltage is seen to have a relatively strong effect on liftoff jet velocity, as expected, suppressing the limit of stability by ~10-15% between 8-12 kV peak-to-peak. The detailed dependence of liftoff jet velocity on voltage amplitude will be discussed in subsequent sections. Using high speed imaging of the flame, we acquired images of flame base position at various points within an AC cycle. Figure 4b is the average of 200 measurements of liftoff height at constant coflow speed and AC frequency, with varying input voltage phase in the SEDD mode. As seen from the graph and also confirmed through a correlation between absolute values of voltage and liftoff height variations (~ -0.25), it is found that the liftoff flame base is not a strong function of the voltage phase. This implies that once a flame is stabilized by a discharge at a certain frequency, then it stably resides near the electrodes regardless of existence of the discharge. This means that at our nominal jet velocity (10 m/s), the input voltage timescale (~33 μs) is much faster than the convective flow timescale (~500 μs) and at least comparable with the recombination timescale of the free electrons.
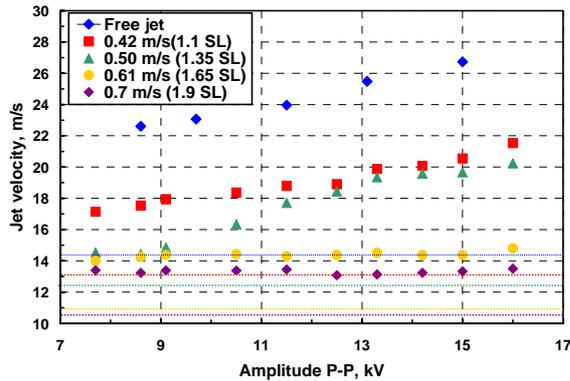
Figure 6. Liftoff jet velocity vs. input P-P voltage with coflow speed as a parameter in SEDD mode. Liftoff jet velocities with no discharge are provided as dotted lines for each coflow speed. Linear and constant relations are observed for low coflow speed and high coflow speed cases, respectively. The electrode position is 10 nozzle diameters downstream (46mm in physical domain).

Figure 5a shows the relation between the maximum coflow speeds avoiding liftoff and the location of the multi-tip circumferential (bare) electrode along the streamwise direction from the nozzle in the SEDD mode. For this experiment, in determining the most appropriate location of electrode, other parameters such as jet velocity, amplitude and frequency of input voltage are held constant. The main observation which can be made from the results of this study is that with all other conditions held constant, there exists a critical coflow speed for flame liftoff stability with the discharge initiated (blue diamond symbols) that is independent of the electrode location, and that is higher than that obtained without the discharge by about 30% (red dotted line). If the laminar flame velocity of methane is used as a reference value, then this corresponds to an increase in velocity of $\sim 0.5\ S_L$ (from 2 S_L to 2.5 S_L). The weak dependence on electrode location was unexpected since the concentration and velocity profiles of the jet are expected to change along the streamwise direction. A possible reason for this behavior is suggested by the results presented in Fig. 5b, where unintensified CCD pictures of the discharge and ensuing flame are presented. The angles that the diffuse current path in the discharge makes relative to the flow direction (see the circles in the picture) appear to change from pointing inwards (left picture) to parallel with the flow (center picture), and finally outwards (right picture) with increasing electrode height. It appears that the discharge adjusts to find the most favorable concentrations and local flow velocity necessary to anchor the flame to the electrode. This finding offers great flexibility in choosing the electrode location without compromising stability limits.

C. Single Electrode Diffuse Discharge (SEDD)

To further evaluate the stabilization capability of the SEDD, the dependence of liftoff jet velocities on varying voltage amplitude was examined (see Fig. 6). At low coflow speeds, such as a free jet (with no coflow) and a jet with $1.1S_L$ of coflow, a linear increase in the critical jet velocity is observed with increasing amplitude. The slope of this increase is more pronounced when the coflow speed is lower. At high levels of coflow such as the $1.6S_L$ and $1.9S_L$ cases, the critical jet velocity is no longer a function of amplitude, but is still strongly dependent on coflow speed. At a moderate coflow speed, $1.35S_L$, a transition from a constant value (independent on amplitude) to linear dependence is observed. In this $1.35S_L$ case, the liftoff jet velocity is equal to the value of the higher ($1.65S_L$) coflow case (yellow circles in Fig. 6) at low amplitudes, but transitions (at an amplitude of about 10 kV) to approach that of the $1.1S_L$ case at higher voltage, suggesting bi-stability. However, in this high voltage amplitude regime, the slope is still less than that of the low coflow case (blue diamonds and red squares in Fig. 6). We attempt to interpret this behavior through a competition between two phenomenon: the counter-acting affect of increased coflow speed on stability, and the enhancing affect of increased discharge intensity at increased voltages. Also, it suggests that once a jet belongs to a coflow-dominant-liftoff regime, then a change in amplitude over a certain range (7.5~16 kV in our case) no longer provides added benefit to stabilization. For comparisons, critical jet velocity values for corresponding coflow speeds without the discharge activated are shown as dotted lines in Fig. 6 (here the colors of the lines match each of the coflow speeds associated with the discharge activated case).

Complementary to Fig. 6, alternative critical jet velocities related to an additional stability criterion -namely blowout - are illustrated as a function of electrode location in Fig. 7. Figure 7a is a schematic diagram to explain the concept of the critical jet velocity. In the event of no plasma discharge, it is well known that liftoff height is an approximately linearly increasing function of jet velocity at fixed coflow speed and also a linearly increasing function of coflow speed at fixed jet velocity as shown as solid black lines in Fig. 7a. However, this dependence becomes more complicated when there is a discharge since the liftoff height depends on additional parameters such as the voltage and characteristic of the discharge. To describe the competition among these parameters, three fundamental observations should be made. First, SEDD is present only when the flame is located in the vicinity of the electrode. In other words, if a flame is lifted off for whatever reason, SEDD disappears and is not reactivated until the flame is brought down and reattached close to the electrode. Inactivation of SEDD in this case is assumed
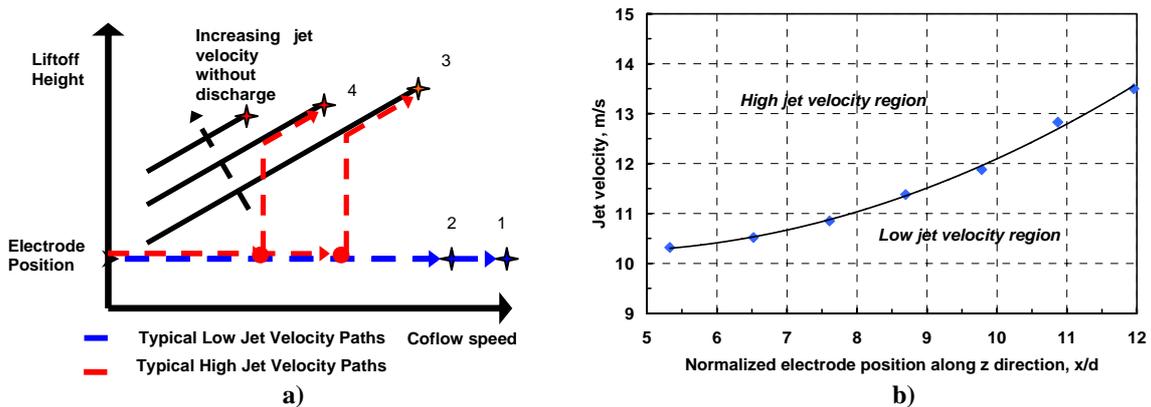
a)   **b)**

Figure 7. Critical blowout jet velocity in SEDD. In a), the concept of the critical blowout jet velocity is described. Blue dotted lines in a) represent typical low jet velocity paths while red dotted lines describe typical high jet velocity paths. The liftoff jet velocities increase with numbers labeled, and a critical jet velocity exists between case 2 and 3. In b), the critical jet velocity is shown for different normalized electrode positions. A region which is lower than the black trend line in b) corresponds to case 1 and 2 while the upper region matches case 3 and 4.

to occur because of the low radical concentration due to the absence of a flame and the high density of surrounding gas owing to low temperature. Second, in case of low jet velocity, a flame is blown out as soon as it is lifted off. Third, a flame is not completely blown out even though it is lifted off when the jet velocity is higher than a critical value. To explain the discrepancy between the second and third observations, competing parameters corresponding to each regime need to be identified.

For the low jet velocity regime, the liftoff must occur once the coflow speed effect surpasses the effect of the discharge because of the negligible contribution of jet velocity to liftoff (blue dotted line). In this case, the coflow speed at this blowout point (blue asterisk) is already higher than a coflow speed without a discharge effect (red asterisk). Furthermore, the discharge itself will disappear due to flame liftoff. Therefore, blowout arises as soon as flame liftoff is reached.

For the high jet velocity regime, the jet velocity is now the main parameter for flame liftoff. Thus, the liftoff can occur by competition between the jet velocity and the discharge effect at a lower coflow speed (red dots) than the no discharge blowout coflow speed (red asterisk). In this case, a flame experiences a sudden jump (red dotted line) to a black solid line, which is the identical location for the case of no discharge. Finally the flame location follows the black solid line rather than the blue line and eventually reaches the red asterisk where blowout occurs with further increase in coflow speed. Therefore, if blowout is the main stabilization criterion rather than liftoff from the electrodes, a maximum jet velocity where the liftoff height does not experience a jump becomes a more important issue. In Fig. 7b, this critical jet velocity is plotted as a function of electrode position. The jet velocities above and below this line represent the high and low velocity cases discussed in Fig. 7a. It is evident that the critical jet velocity increases with increasing electrode height because local jet velocities decrease with increasing electrode height.
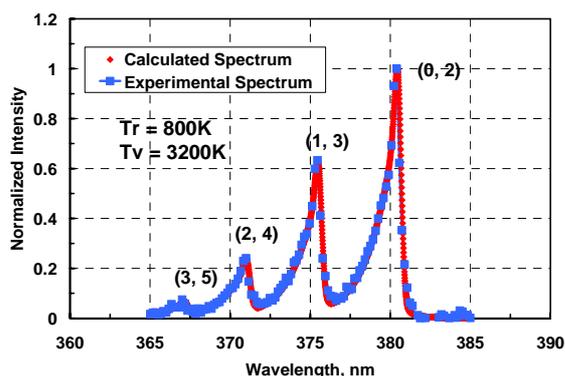

Figure 8. 2nd positive vibrational band spectra of Nitrogen with $\Delta v = 2$ measured in the DBD. Blue squares represent experimental values. For comparison, red diamonds are calculated values at a specific rotational and vibrational temperature.

D. Dielectric Barrier Discharge

It is expected that the thermodynamic state of either the SEDD or the DBD discharge is highly non-equilibrium. To investigate and confirm the non-equilibrium state of our DBD, we characterized the emission spectra of the 2nd positive system of molecular

7
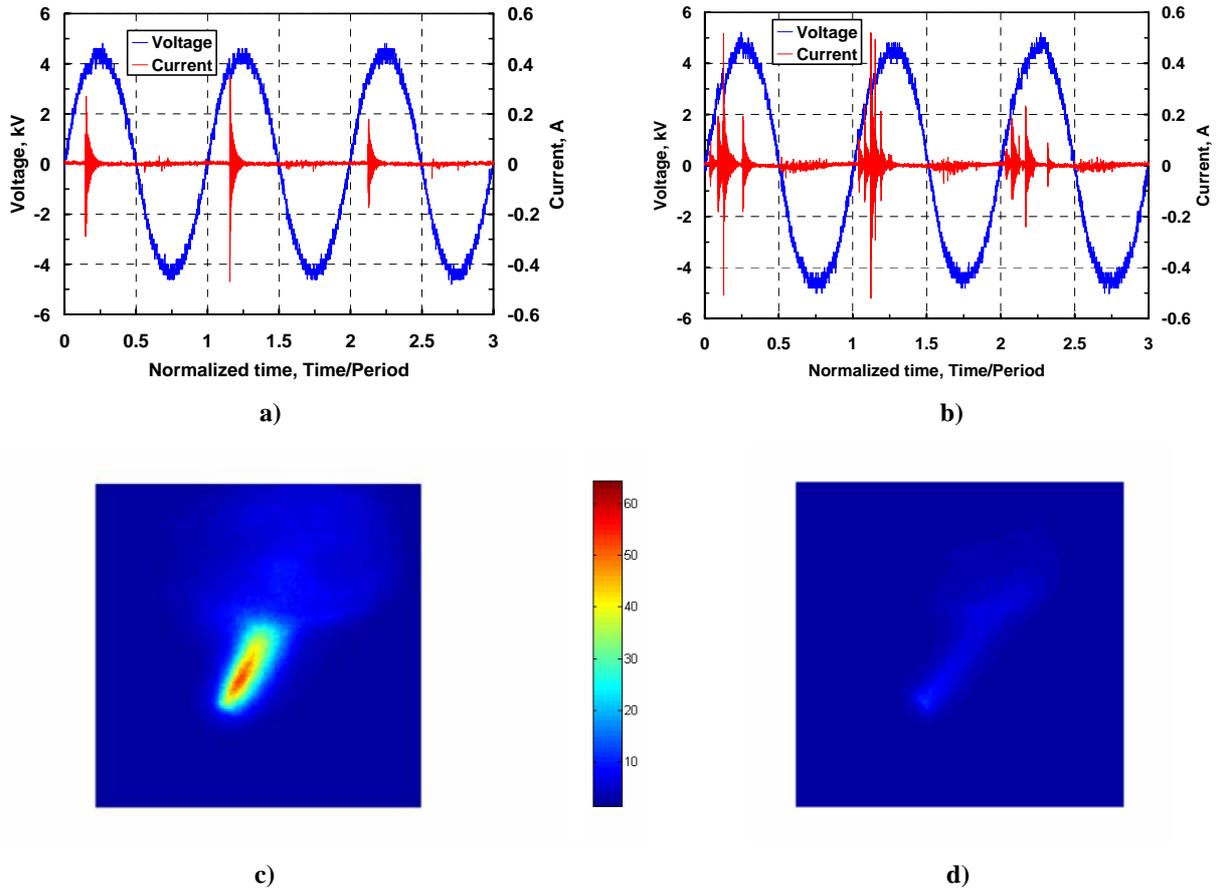American Institute of Aeronautics and Astronautics

Figure 9. Voltage and current characteristic of the DBD. a) Single-needle discharge. b) multiple-needle discharge. An asymmetric discharge tendency depending on the polarity of voltage is observed in a) and b), and is confirmed in intensified images of discharge in c) (positive polarity) and d) (negative polarity). For c) and d), 2ns of gating time and 20000 shots of on-chip accumulation are used.

nitrogen, namely the $C^3\Pi_u \rightarrow B^3\Pi_g$, $\Delta\upsilon = 2$ transition, since this $\Delta\upsilon = 2$ transition has clearly resolved vibrational bands compared to $\Delta\upsilon = 0,1$ transitions and its intensity is relatively strong compared to higher $\Delta\upsilon$ bands. The obtained spectra are used to determine vibrational and rotational temperatures by comparing those measured with calculated spectra at specific temperatures. In modeling the spectrum, we make two assumptions: first, rotational energy transfer (RET) and vibrational energy transfer (VET) are assumed fast enough so that rotational and vibrational temperatures are in partial equilibrium, characterized by their own unique temperatures. Second, equilibrium between rotational and vibrational modes may not necessarily be reached due to the short time scales associated with the discharge. The results from preliminary measurements confirm the existence of a strong non-equilibrium flow, with the model fit to the measured spectra indicating a temperature of 800K for the rotational mode and 3200K for the vibrational mode. The comparison between calculated and experimental spectra is shown in Fig. 8. The uncertainty in the established rotational temperature of ~200K is due mainly to the limited resolution of the spectrometer employed in these studies, characterized by calibration with a Hg vapor discharge lamp. It is expected that the rotational temperature is strongly representative of the translational temperature of the flow due to an expected rapid energy transfer between these modes. Although we have not yet modeled the implication that this degree of non-equilibrium may have on the flame kinetics, it is expected that the high vibrational temperature associated with molecular nitrogen channels energy into dissociation of molecular oxygen[5], leading to the formation of a rich pool of radical species that can accelerate flame reactions without raising the overall flow temperature.

With the circumferential multi-tipped electrode, the number of tips actively collecting current is found to depend on the discharge amplitude, as confirmed through direct imaging, and by examination of the current and voltage waveforms. Typical voltage and current waveforms for the discharge are illustrated in Fig. 9. Figure 9a represents a
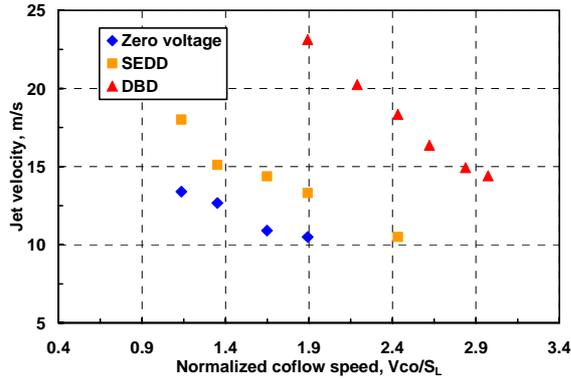
American Institute of Aeronautics and Astronautics

Figure 10. The improvement of liftoff jet velocity as a function of normalized coflow speed. Stability limits are extended to 2.5S_L and 3S_L with SEDD and DBD, respectively. The input P-P voltage is 9.35kV and the frequency is 30kHz. The electrode position is fixed at 10 nozzle diameters (46mm above the nozzle).

low power case with only one active tip while Fig. 9b corresponds to a high power case that has multiple active tips. Some observations can be made by inspection of these waveforms. First, as expected, the discharge pulse width is much smaller compared to the period of an input AC voltage, characteristic of a dielectric barrier discharge. Second, the discharge current is dependent on the polarity of the voltage, which is in contrast with previous conventional DBD observations[16] and simulations[17], most likely due to the asymmetry of the electrode configuration used in our studies. Finally, as the discharge power (voltage) is increased slightly (Fig. 9b), additional tips become active, and the associated current spikes tend to be randomly distributed in time about a mean phase of about 45° within the positive voltage swing in the first quadrant of the AC cycle. The tendency to discharge during the positive cycle of the AC waveform can also be seen in intensified images of the discharges. In Figs. 9c and 9d, 20,000 ensemble-averaged images of a typical discharge during the positive polarity phase and negative polarity phase, respectively, are illustrated. It is apparent that an intense filamentary discharge is formed between the tip electrode and the quartz-covered circumferential (grounded) electrode during the positive phase of the cycle (Fig. 9c). Not as apparent is the presence of a weak glow discharge surrounding the quartz envelope. A much less intense discharge is observed during the negative phase of the discharge cycle (Fig. 9d). It is noteworthy that both images share identical color scales and camera gating times (2 ns).

The dramatic enhancement in flame stabilization due to the AC discharge is summarized by the data in Fig. 10. Here the coflow speed is used as a variable against which the critical jet velocity for liftoff is compared. It appears that the DBD mode shows much promise in enhancing flame stability, most likely due to its ability to support a higher discharge current density. A further advantage of the DBD mode is that it can be sustained in the absence of the flame, in contrast to the SEDD mode, where the flame serves as a virtual ground electrode. It is noteworthy that the maximum coflow speed in which the flame is stably anchored to the electrode can be extended to around 3S_L even with just a modest discharge power of 0.5W - only approximately 0.005% of the rate of energy released by the flame itself. However, we must also note that SEDD may be an attractive alternative configuration as it consumes less power, and does not require the second electrode. While the limits of the stabilization afforded by the SEDD mode does fall short of that of the DBD mode, it nonetheless extends the liftoff limits by 20-30%, warranting further studies.

IV. Conclusions

We have reported on the use of two different types of AC discharges in enhancing the stability of a non-premixed lifted jet flame. The behavior of a Single Electrode Diffuse Discharge (SEDD) and a Dielectric Barrier Discharge (DBD) driven by a conventional AC power supply were compared. The electrode configuration examined here, and proposed for further studies is of an axisymmetric design to minimize the disturbance of the flame structure. The driven (bare) electrode has multiple platinum tips for distributed current flow. It is found that the electrode positions and AC source frequency are not critical factors affecting flame stability. The insensitivity to electrode position is surprising, and is attributed to the tendency of the discharge (in the SEDD mode) to find the most favorable conditions necessary to anchor the flame to the electrodes. In the SEDD mode, and at moderate jet velocity, flame liftoff is suggested to be determined by a competition between coflow speed and discharge intensity (voltage). At higher jet velocity, jet-driven liftoff is found to occur at a critical jet velocity. A major accomplishment in these studies is that the coflow speed was increased to 2.5S_L at maximum stabilization, with very modest investments in discharge power. We believe that the DBD mode can be even more effective in flame stabilization, perhaps capable of increasing coflow speed limits to 3S_L. A quantitative analysis of the molecular nitrogen emission confirmed the highly non-equilibrium nature of these atmospheric pressure discharges, with a rotational temperature (which is expected to be close to the translational temperature) of approximately 800K and a vibrational temperature of 3200K. The non-equilibrium offers a robust path for energy transfer into dissociation processes, which can create

a rich pool of oxygen radicals needed to promote flame anchoring to the electrodes. This work describes our preliminary study of implementing plasma discharges for enhancing flame stability. While we have promising results indicating that these SEDD and DBD configurations can be effective in flame stabilization, the results presented here are limited to lifted jet flames in coflow geometry. Efforts are presently underway to extend our investigation to premixed flames, nitrogen diluted flames and to jets in crossflow flame configurations.

Acknowledgments

References

[1] Muñiz, L., Mungal, M.G. (2001), "Effects of Heat Release and Buoyancy on Flow Structure and Entrainment in Turbulent Nonpremixed Flames," Comb. Flame, 126, 1402-1420.

[2] Han, D., Mungal, M.G., "Simultaneous Measurement of Velocity and CH Layer Distribution in Turbulent Non-premixed Flames, *Proceedings of the Combustion Institute*, Vol. 28, 2000, pp. 261-267.

[3] Carter, C.D., Donbar, J.M., Driscoll, J.F., "Simultaneous CH-PIV Imaging of Turbulent Nonpremixed Flames," *Applied Physics B,* Vol. 66, 1998, pp. 129-132.

[4] Schefer, R.W., Namazian, M., Kelly, J, "Velocity Measurements in a Turbulent Nonpremixed Bluff-Body Stabilized Flame," *Combustion Science and Technology,* Vol. 56, 1987, pp 101-138.

[5] Bozhenkov, S.A., Starikovskaia, S.M., Starikovskii, A.Yu., "Chemical Reactions and Ignition Control by Nanosecond High-Voltage Discharge," *11th AIAA/AAAF International Conference,* AIAA-2002-5185, 2002.

[6] Vervisch, P., Personal Communication

[7] http://www.onera.fr/seminaires/plasmas/onera-cnrs-030331.html

[8] Starikovskii, A.Yu., "Plasma Supported Combustion," *Proceedings of the Combustion Institute,* 30th International Symposium on Combustion, Chicago, 2004, pp. 326.

[9] Schoenbach, K.H., El-Habachi, A., Shi, W., Ciocca, M., "High-pressure Hollow Cathode Discharges," *Plasma Sources Sci. Technol.,* Vol. 6, 1997, pp. 468-477

[10] Moselhy, M., Petzenhauser, I., Frank, K., Schoenbach, K.H., "Excimer Emission from Microhollow Cathode Argon Discharges," *Journal of Physics D: Applied Physics,* Vol. 36, 2003, pp. 2922-2927

[11] Packan, D., "Repetitive Nanosecond Glow Discharge in Atmospheric Pressure Air," Ph.D. Dissertation, TSD-152, Mechanical Engineering Dept., Stanford Univ., Stanford, CA, 2003.

[12] Ko, Y.S., Chung, S.H., Kim, G.S., Kim, S.W., "Stoichiometry at the Leading Edge of a Tribrachial Flame in Laminar Jets from Raman Scattering Technique," *Combust. Flame,* Vol. 123, 2000, pp. 430-433.

[13] Joedicke, A., Peters, N., Mansour, M., "The Stabilization Mechanism and Structure of Turbulent Hydrocarbon Lifted Flames," *Proceedings of the Combustion Institute,* 30th International Symposium on Combustion, Chicago, 2004.

[14] Han. D., Mungal, M.G., "Observations on the Transition from Flame Liftoff to Flame Blowout," *Proceedings of the Combustion Institute,* 28th International Symposium on Combustion, Edinburgh, 2000, Vol. 28, pp. 537-543.

[15] Muñiz, L., Mungal, M.G. "Instantaneous Flame-stabilization Velocities in Lifted-jet Diffusion Flames," *Comb. Flame,* Vol. 111, 1997, pp. 16-31.

[16] Okazaki K., Nozaki, T., "Ultrashort Pulsed Barrier Discharges and Applications," *Pure and Applied Chemistry,* Vol. 74, 2002, pp. 447-452.

[17] Boeuf, J.P., Pitchford, L.C., Callegari, Th., "Basic Properties of Micro-Discharges in Dielectric Barrier and Hollow Cathode Configurations," *Proceedings of the 2nd International Workshop on Microplasmas*, Hoboken, 2004.